



ORIGINAL ARTICLE

Spectroscopic and TDDFT studies of N-phenyl-N'-(3-triazoly)thiourea) compounds with transition metal ions



Ahmed M. Mansour^{1,*}, Ola R. Shehab¹

Department of Chemistry, Faculty of Science, Cairo University, Gamma Street, Giza 12613, Egypt

Received 11 September 2020; accepted 3 December 2020

Available online 9 December 2020

KEYWORDS

Antibacterial activity;
NBO;
TDDFT;
Thiourea ligands;
Triazole

Abstract Reaction of N-phenyl-N'-(3-triazoly)thiourea (H_3L) with $M(ClO_4)_2$ ($M = Co(II)$ (**1**), $Ni(II)$ (**2**) and $Cu(II)$ (**3**)) afforded $[M(H_2L)_2]$ complexes, which were characterized experimentally and theoretically using different analytical, and spectral tools. The susceptibility of *Staphylococcus aureus* and *Escherichia coli* bacteria towards H_3L and its complexes was evaluated. The thiourea ligand coordinates to the 3d-metal ions via $C-S^-$, and triazole nitrogen yielding coordination compounds between the tetrahedral, and square-planar geometries (“flattened” tetrahedron, D_{2d} symmetry). Full geometry optimization, vibrational analyses, and natural bond orbital analyses of the proposed conformations of **1–3** were executed at B3LYP/def2-SVP to gain some knowledge about the local minima structures, natural charge of the coordinated metal ion, electronic configuration as well as the hybridization of M–L bonds. The electronic structures of the local minimum structures of **1–3** were investigated by time-dependent density functional theory calculations. Coordination of the thiourea ligand to $Co(II)$ and $Cu(II)$ ions did alter the toxicity against the tested microbes, while chelation of $Ni(II)$ ion gave rise to inactive species.

© 2020 Published by Elsevier B.V. on behalf of King Saud University. This is an open access article under the CC BY-NC-ND license (<http://creativecommons.org/licenses/by-nc-nd/4.0/>).

1. Introduction

The coordination chemistry of thiourea, and their derivatives received considerable interest due to their valuable industrial, (Fuerst and Jacobsen, 2005; Khaled, 2009; Fontás et al., 2005) and biological applications. (Zhao et al., 2009; Sunduru et al., 2009; Han et al., 2006; Mansour, 2016; Manjula et al., 2009; Dixit et al., 2006) Metal complexes of some thiourea derivatives exhibited effective anti-inflammatory, (Zhao et al., 2009) antimalarial, (Sunduru et al., 2009) antimicrobial (Han et al., 2006; Mansour, 2016) and cytotoxic activities. (Manjula et al., 2009; Dixit et al.,

* Corresponding author.

E-mail addresses: mansour@sci.cu.edu.eg (A.M. Mansour), Olashehab@sci.cu.edu.eg (O.R. Shehab).

¹ The authors have equal contribution to the present work.

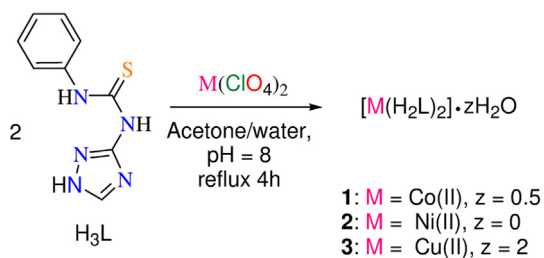
Peer review under responsibility of King Saud University.



2006) Urease, the nickel-containing metalloenzyme, catalyzes the hydrolysis of urea in some plants and animals forming ammonia and CO₂. Subsequently, some thiourea based Ni (II) complexes were investigated as models for the nickel center of enzymes. (Halcrow and Christou, 1994) Some thiourea derivatives exhibited respectable inhibitory activity towards tyrosine kinases, protein tyrosine kinases, and NADH oxidase (Hubbard and Till, 2000). Alternatively, the applications of thiourea based compounds were extended to cover the areas of catalysis, (Fuerst and Jacobsen, 2005) corrosion inhibitors, (Khaled, 2009) and water treatment to remove the heavy metal ion. (Fontás et al., 2005) Some thiourea derivatives were investigated and used as ionophores for anion sensing. (Liu et al., 2005; Blažek Bregovic et al., 2015) Photoactivatable properties of tricarbonyl thiourea manganese(I) compounds, capable of releasing CO upon the irradiation at 525–468 nm, were recently reported. (Mansour and Shehab, 2018; Mansour and Friedrich, 2017) The combination of soft chelation thione group and strong σ -donating ligand, Br⁻ weaken the Mn–CO bond and facilitated the CO release. “Piano-stool” Ru (η^6 -*p*-Cym)²⁺ complexes functionalized with thiourea derivatives exhibited excellent toxicity to *Staphylococcus aureus*, which influenced by the type of the heterocyclic arm. (Mansour and Radacki, 2020) On the other hand, triazole-based compounds showed significant biological activity as antifungal, (Papakonstantinou-Garoufalas et al., 1998) and antimicrobial agents (Colanceska-Ragenovic et al., 2001).

In the present contribution, it is motivating to include triazole moiety into the framework of thiourea *via* the synthesis of N-phenyl-N'-(3-triazolyl)thiourea (H₃L, Scheme 1). The crystal structure, and the antimicrobial properties of H₃L were reported by Stefanska et al. (2012). H₃L ligand plays an important role in inhibition of the enzymatic properties of copper-containing enzyme, Dopamine β -hydroxylase (DBH), (Goldstein et al., 1965) which is essential to catalyze the final step of the conversion of dopamine to norepinephrine Cl, through the uptake of the copper from the DBH enzyme. Coordination of H₃L to Pd(II) and Pt(II) ion gave rise to inactive species. (Mansour, 2018) The solid metal complexes of H₃L with Co(II), Ni(II), Cu(II), and Cd(II) chlorides were reported elsewhere (Salman, 2001) assuming that H₃L behaved as a neutral bidentate ligand towards the latter mentioned Mⁿ⁺ ions *via* the thione, and triazole nitrogen that is inconsistent with our findings.

Herein, the ligational behavior of H₃L towards some 3d-transition metal ions was investigated both experimentally, and theoretically using different analytical and spectroscopic tools. Afterward, geometry optimization, and vibrational analyses of the proposed structures of 1–3, in the ground state,



Scheme 1 Synthesis of some thiourea based 3d-transition metal complexes 1–3.

were performed to obtain some knowledge about the local minima structures. Natural bond orbital analyses (Reed et al., 1988) were executed to obtain some information about the intramolecular H-bond interactions, hybridization of M–L bonds, electronic configuration, and charge of the coordinated metal ion. To understand the observed absorption electronic transitions, time-dependent density functional theory (TDDFT) calculations were performed. Finally, the antibacterial activity of the compounds was assessed against *Staphylococcus aureus* and *Escherichia coli*.

2. Experimental section

2.1. General procedures

Phenyl isothiocyanate, 2-amino-1,3,4-triazole, pyridine, metal perchlorates (Co(ClO₄)₂·6H₂O, Ni(ClO₄)₂·6H₂O, and Cu(ClO₄)₂·6H₂O) and organic solvents were purchased from the commercial sources and used as received. The thiourea ligand was prepared by following the previously reported method. (Mansour, 2018) Potassium bromide pellets of the ligand and complexes were subjected to IR analysis using *Jasco FTIR 460 plus*. Micro-elemental analyses were determined on an Automatic Analyzer CHNS, *Vario EL III Elementar*. Electronic absorption spectra were recorded on *OPTIZEN POP* automate spectrophotometer. The magnetic susceptibility values of the paramagnetic complexes were determined using Sherwood scientific magnetic balance using Gouy method. (Hilal and Fredericks, 1954) The molar conductivity values were obtained by *digital Jenway 4310* (cell constant is 1.02). X-band EPR measurements were executed on solid samples at 298 K using a Bruker EMX spectrometer. The magnetic modulation frequency was 100 kHz, and the microwave power was set to 0.201 mW. The *g*-values were recorded by referencing to a diphenylpicrylhydrazyl (DPPH) sample with *g* = 2.0036. The modulation amplitude was fitted at 4 Gauss while the microwave frequency was verified as 9.775 GHz. Thermogravimetric analysis (TGA) was executed under dinitrogen atmosphere (20 mL min⁻¹) in platinum crucible with a heating rate of 10 °C min⁻¹ using a *Shimadzu DTG-60H simultaneous DTG/TG* apparatus.

2.2. Synthetic procedures

To a round flask charged with H₃L ligand (2 mmol, 436 mg), and acetone (20 mL), 5 mL aqueous solution of metal perchlorate (1 mmol; Co(ClO₄)₂·6H₂O (365 mg), Ni(ClO₄)₂·6H₂O (366 mg) and Cu(ClO₄)₂·6H₂O (370 mg) was added and then the pH of the reaction mixtures was adjusted at around 8.0 by adding few drops of ammonia. Then the solutions were heated to reflux for 4 h, whereupon precipitation occurred. The solid products were collected by filtration, washed with diethyl ether, and dried under vacuum. Stock solutions (10⁻³ M) of complexes 1–3 (Scheme 1) in DMF were prepared and their molar conductance values were recorded and compared to the reported data for 1:1 (65–90 Ω⁻¹ cm² mol⁻¹) and 1:2 (130–170 Ω⁻¹ cm² mol⁻¹) electrolytes in the same solvent at the same temperature. (Mansour, 2014) The conductance values of 1–3 were found to be in the range of 13.8–41.2 Ω⁻¹ cm² mol⁻¹ reflecting the non-ionic nature of the complexes and rules out the probab-

ity of presence of the perchlorate ion(s) in the secondary coordination sphere.

- [Co(H₂L)₂].0.5H₂O (**1**): Brown, yield 75% (759 mg, 1.5 mmol). IR (FTR, cm⁻¹): $\nu = 3399$ (br, NH), 3211 (br, NH), 3024 (w, CH), 1563 (w, -S-C = N^{-thiol}/CC), 1520 (w, CC), 1487, 1397, 1310 (m, C^{-N}/C^{-S}/C-H ^{β}), 1257, 1173, 1083 (br, C-N/C^{-S}), 754 (m, C^{-S}). C₁₈H₁₆CoN₁₀S₂.0.5H₂O: C 42.86, H 3.40, N 27.77, found C 43.22, H 3.44, N 27.92. UV/Vis (DMF, 10⁻⁴ M, nm): 260, 280, 570. ESI-MS (positive mode, acetone): 496.0558 {M + 1}⁺ (M: molecular mass). Effective magnetic moment, μ_{eff} (μ_{B} , 298 K): 2.79. Molar conductance (DMF, 10⁻³ M, $\Omega^{-1}\text{cm}^2\text{mol}^{-1}$): 41.2.
- [Ni(H₂L)₂] (**2**): Buff, yield 79% (788 mg, 1.57 mmol). IR (FTR, cm⁻¹): $\nu = 3386$ (br, NH), 3228 (br, NH), 3030 (w, CH), 1594 (m, -S-C = N^{-thiol}), 1530 (w, CC), 1494, 1396, 1311 (m, C^{-N}/C^{-S}/C-H ^{β}), 1209, 1086 (br, C-N/C^{-S}), 747 (m, C^{-S}). C₁₈H₁₆NiN₁₀S₂: C 43.66, H 3.26, N 28.28, found C 43.22, H 3.28, N 27.92. UV/Vis (DMF, 10⁻⁴ M, nm): 255, 295, 370, 445. ESI-MS (positive mode, acetone): 494.0935 {M + 1}⁺. μ_{eff} (μ_{B} , 298 K): 0.78. Molar conductance (DMF, 10⁻³ M, $\Omega^{-1}\text{cm}^2\text{mol}^{-1}$): 13.8.
- [Cu(H₂L)₂].2H₂O (**3**): Dark-brown, 76% (812 mg, 1.51 mmol). IR (FTR, cm⁻¹): $\nu = 3399$ (br, NH), 3299 (br, NH), 3026 (w, CH), 1572 (w, -S-C = N^{-thiol}/CC), 1493, 1361, 1313 (m, C^{-N}/C^{-S}/C-H ^{β}), 1259, 1096 (br, C-N/C^{-S}), 743 (m, C^{-S}). C₁₈H₁₆CuN₁₀S₂.2H₂O: C 40.33, H 3.76, N 26.13, found C 40.32, H 3.44, N 25.85. UV/Vis (DMF, 10⁻⁴ M, nm): 300, 335, 390, 405, 470, 620. ESI-MS (positive mode, acetone): 501.1330 {M + 1}⁺. μ_{eff} (μ_{B} , 298 K): 1.44. Molar conductance (DMF, 10⁻³ M, $\Omega^{-1}\text{cm}^2\text{mol}^{-1}$): 20.3.

2.3. DFT/NBO/TDDFT calculations

Full geometry optimization of the proposed four-coordinated conformations of **1–3**, in the ground state, and their vibrational analyses were carried out by Becke 3-parameter (exchange) Lee–Yang–Parr (B3LYP) functional, (Becke, 1993) and def2-SVP basis set using Gaussian03 package (Frisch et al., 2003). For time dependent density functional theory (TDDFT) calculations, the 30 singlet excited states were considered and calculated at CAM-B3LYP (with long range correction) (Yanai et al., 2004)/def2-SVP level of theory. Dimethyl sulfoxide was incorporated in the TDDFT calculations using the polarized continuum model as implemented in Gaussian03. Natural population analyses were executed using NBO method at B3LYP/def2-SVP level of theory. Local minimum structures, electronic spectra, and frontier molecular orbitals were visualized by Gaussview03 (Frisch et al., 2000).

2.4. Antibacterial activity

The antibacterial activities of the functionalized thiourea ligand and its coordination compounds against cultures of *Staphylococcus aureus* and *Escherichia coli* microbes were assessed using a modified Kirby–Bauer disc diffusion method (Abdel-Ghani and Mansour, 2012) at the concentration of 20 mg mL⁻¹, while keeping the final DMSO concentration to a maximum of

0.5% and serially diluted 1:2 fold for 8 times. The toxicity of the compounds was compared to the standard tetracycline. In this assay, the centrifuged pellets of bacteria from a 24 h old culture comprising of approximately 10⁴–10⁶ CFU mL⁻¹ (CFU: colony forming unit) were distributed on the surface of Mueller–Hinton Agar plates (evaluated for composition and pH). Then, the wells were contaminated with 10 mL of prepared inocula to get 10⁶ CFU mL⁻¹. Petri plates were made by flowing 100 mL of seeded nutrient agar. Plates were covered and incubated at 37 °C for 18 h. DMSO (0.1 mL) was used as control under the same conditions for each microorganism, subtracting the diameter of the inhibition zone obtained with the solvent from that observed in each case. The antibacterial activities were determined as a mean of three replicates.

3. Results & discussion

3.1. Synthesis and spectral characterization

The transition metal complexes **1–3** (Scheme 1) were prepared by heating to reflux the slightly alkaline reaction mixtures of the metal perchlorates and H₃L, in 75% (v/v) acetone–water mixture, where complexes [M(H₂L)₂] (M = Co(II) (**1**), Ni(II) (**2**) and Cu(II) (**3**)) were collected by filtration. Their proposed structures were deduced from elemental analysis, TGA, UV/Vis, IR, ESR, magnetic and conductivity measurements. The vibrational spectrum of the free ligand (Fig. S1) shows two broad bands at 3381, and 3207 cm⁻¹ assigned to the $\nu(\text{NH})^{\text{Ph}}$ and $\nu(\text{NH})^{\text{triazole-exo}}$ modes as well as a group of bands in the range of 1570–700 cm⁻¹ having a contribution from -NH-C = S group as follows: 1540 ($\beta(\text{N-H})/\beta(\text{C} = \text{C})$) **I**, 1385 ($\nu(\text{C}^{\text{-N}})/\nu(\text{C} = \text{S})/\beta(\text{C-H})$) **II**, 1018 ($\nu(\text{C-N})/\nu(\text{C-S})$) **III**, and 837 cm⁻¹ ($\delta(\text{C} = \text{S})$) **IV** (Mansour, 2016; Mansour, 2018). The $\nu(\text{NH})^{\text{triazole-endo}}$ could not be identified owing to the tautomeric structure of the triazole ring. The absence of $\nu(\text{S-H})$ mode at around 2570 cm⁻¹ in the IR spectrum of the free ligand as well as the presence of a signal at δ 177.0 ppm in the ¹³C NMR spectrum confirm the existence of H₃L in the thione form in both the solution and solid states. Coordination of H₃L to the metal ion induced considerable spectral changes in the vibrational ranges of 1630–1300, and 900–700 cm⁻¹. A new band assigned to $\nu(\text{S-C} = \text{N}^{\text{thiol}})$ at 1594 cm⁻¹ in the spectrum of **2** or allocated for $\nu(\text{S-C} = \text{N}^{\text{thiol}})/\nu(\text{CC})$ at 1563 and 1572 cm⁻¹ in the spectra of **1**, and **3** is observed, which may be attributed to enolization of -NH-C = S group into -N = C-SH, ionization of SH group, and coordination to metal ion (Fig. S1). The shift of $\nu(\text{NH})^{\text{Ph}}$ mode to higher wave numbers (3386–3399 cm⁻¹) rules out the role of the phenyl-NH group in the metal complex formation. The participation of the triazole nitrogen in the chelation inhibits the tautomeric behaviour within the moiety and leads to grown of a new band in the range of 3299–3211 cm⁻¹ assigned to the $\nu(\text{NH})^{\text{triazole-endo}}$ mode. IR studies indicated that the H₃L coordinates to Mⁿ⁺ via C-S⁻, and triazole nitrogen.

The electronic absorption spectrum of the free ligand, in DMF, (Fig. S2) displays two electronic transitions at 271, and 310 nm (Mansour, 2018). In the highest energy region of the electronic spectrum of **1**, two prominent bands corresponding to the intra-ligand transitions are observed at 260 and 280 nm. In addition, a broad shoulder is seen at around

570 nm in the spectrum of **1** (Fig. S2), which may be assigned to ${}^4A_2 \rightarrow {}^4T_1(P)$ (v_3) in tetrahedral Co(II) geometry (Kowalkowska-Zedler et al., 2020; Vařák et al., 1981). The effective magnetic moment of **1** is $2.79 \mu_B$. Generally, octahedral Co(II) complexes exhibit μ_{eff} values around $4.7 \mu_B$ owing to the large orbital contribution, while the square-planar complexes show values around $1.7 \mu_B$ corresponding to presence of an unpaired electron. Tetrahedral Co(II) complexes have μ_{eff} values usually equivalent to the population of three unpaired electrons that may be affected by orbital contribution. The observed μ_{eff} of **1** further complements the electronic findings of the distorted tetrahedral field. The μ_{eff} value of **2** is $0.78 \mu_B$ suggesting a highly probability of presence of a mixture of square-planar/tetrahedral (Al-Awadi et al., 2006; Kandil et al., 2002) or existence of Ni(II) ion in a flattened tetrahedral field. By assuming the presence of a mixture of the two four-coordinated geometries, the tetrahedral percentage (N_t) in the proposed mixture is 5.6% according to the following relation, $N_t = [(\mu_{\text{eff}})^2 / (3.3)^2] \times 100$, where μ_{eff} value for ideal tetrahedral Ni(II) complexes is $3.3 \mu_B$. The electronic spectrum of **2** shows four transitions at 255, 295, 370, and 445 nm (Fig. S2). The two highest energy bands at 255, and 295 nm are assigned to $\pi \rightarrow \pi^*$ transitions within the ligand framework. The shoulder at 370 nm is allocated for LMCT ($S(\sigma) \rightarrow \text{Ni(II)}$) and the broad band at 445 nm is assigned to a combination of LMCT ($N(\sigma) \rightarrow \text{Ni(II)}$)/ $d_{z^2} \rightarrow d_{x^2-y^2}$ (${}^1A_{1g} \rightarrow {}^1B_{1g}$) transitions (Royer et al., 1972). For Cu(II) complex **3**, the μ_{eff} ($1.44 \mu_B$) is slightly lower than the expected value for the regular spin only value of d^9 metal ion revealing the probability of presence of weak anti-ferromagnetic interactions between the neighbouring species (Mansour, 2013). The electronic absorption spectrum of **3** (Fig. S2), in DMF, is characterized by four transitions in the visible region at 390, 405, 470, and 620 nm. Generally, square-planar Cu(II) coordination compounds are characterized by a broad band at around 650 nm corresponding to the unresolved d-d transitions, while tetrahedral complexes have no electronic transitions in the 500–1000 nm region (Sreekanth and Prathapachandra-Kurup, 2003). The transitions at 405, 470, and 620 nm may be assigned to LMCT ($S(\sigma) \rightarrow \text{Cu(II)}$) (Dhara et al., 2004), LMCT($N(\pi) \rightarrow \text{Cu(II)}$) (Sreekanth and Kurup, 2003) and $d_{xz}/d_{yz}/d_{z^2} \rightarrow d_{x^2-y^2}$ (${}^2B_{1g} \rightarrow {}^2E_{1g}$ and ${}^2B_{1g} \rightarrow {}^2A_{1g}$) (Lever, 1984; Garg et al., 1993) within the square-planar field. Therefore, in the solution state, Cu(II) ion of **3** may be surrounded by four ligands, which are arranged in a planar form.

The thermal decompositions of complexes (**1–3**) were examined in the temperature range from the ambient up to 1000°C , under pure dinitrogen atmosphere, using a heating rate of $10^\circ\text{C}/\text{min}$ (Fig. S3). For **1**, the decomposition starts at about 50°C and proceeds through three complicated thermal steps maximally at 79, 283, and 489°C . The first step is accompanied by a mass loss of 1.67% (calcd. 1.79%) corresponding to desorption of $0.5\text{H}_2\text{O}$. The thermal steps bring the total mass loss up to 65.45% (calcd. 66.20%) leaving carbonized CoS_2 (Mansour, 2014). In the case of **2**, no thermal decomposition is observed below 130°C revealing the absence of any volatile solvents and/or water of hydration. The thermogravimetric analysis of **2** shows four stages maximally at 242, 416, 488, and 782°C . For **3**, the mass loss has been taken in four thermal steps maximally at 77, 189, 238, and 484°C . The first thermal stage up to 110°C , with a mass loss of 6.52% (calcd.

6.71%), may be attributed to desorption of two hydrated water molecules. It seems that compounds **2** and **3** are hardly to be decomposed in the temperature range up to 1000°C under an inert atmosphere with a total mass loss of 54.61% and 58.22%, respectively, as no plateau is reached and no stable Ni(II) or Cu(II) residue may be proposed to be existed at 1000°C . This behaviour has been reported with similar complexes under the same experimental conditions (Mansour, 2016; Faraglia et al., 1990).

The solid-state X-band EPR spectrum of Cu(II) complex **3** (Fig. 1), at the room temperature is axial with two well defined $g_{\parallel} = 2.30$ ($A_{\parallel} = 129 \times 10^{-4} \text{cm}^{-1}$) and $g_{\perp} = 2.05$ values and $g_{\parallel} > g_{\perp} > g_e$ (2.0023) indicating that the unpaired electron may be present in the $d_{x^2-y^2}$ orbital. The degree of the distortion from the tetrahedral geometry can be deduced from the f value ($g_{\parallel}/A_{\parallel}$), where $f = 105\text{--}135 \text{cm}$ is recognized for the idea square-planar geometry and $f > 135 \text{cm}$ indicates the presence of a distorted tetrahedral geometry (Sundaravel et al., 2009). It is worthy mention that the f value of **3** is 178cm suggesting presence of Cu(II) ion in the tetrahedron field in the solid state, and this has been further supported by quantum chemical calculations (*vide infra*).

The spectroscopic, magnetic, and analytical data of the complexes, prepared from the reaction of H_3L , and metal perchlorate salts in a slightly basic media, indicated the formation $[\text{M}(\text{H}_2\text{L})_2]$ compounds. Searching in the literature showed that the reaction between H_3L and metal chloride salts afforded compounds of the type $[\text{M}(\text{H}_3\text{L})_n\text{Cl}_2]$ ($\text{M} = \text{Co(II)}, \text{Ni(II)}, \text{and Cu(II)}$; $n = 1$ and 2). (Salman, 2001) In comparison, changing of the experimental conditions e.g. pH of the medium, and/or using of metal salts of weakly coordinating anions e.g. ClO_4^- affect the coordinating ability of our tribasic ligand, and increase the probability of the departure of the anions of the metal salts from the coordination spheres of the complexes compared to the published complexes, which were prepared from the same ligand, but with different metal salts and experimental conditions.

3.2. DFT/NBO analysis

In the previous section, the analytical and spectroscopic data indicated that compounds **1–3** are present in a "flattened" tetrahedron field, in which the thiourea ligand coordinates to the title metal ions, as a mono-negatively bidentate ligand,

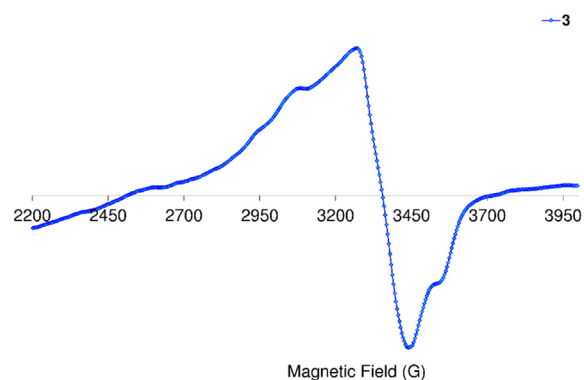


Fig. 1 EPR spectrum of Cu(II) complex, **3**.

via C-S⁻, and triazole nitrogen. However, there is still two questions that have not been experimentally answered as follows: which nitrogen of the triazole ring is involvement in the complex formation (N(1) vs. N(3))? and which geometrical isomer (*cis*- vs. *trans*-) is the local minimum structure of the complex?. To address these two questions, full geometry optimizations of the proposed structures of **1**–**3**, in the ground state, were executed at B3LYP/def2-SVP level of theory. As shown in Table 1, conformations **I**, and **II** have been assigned to the *trans*- and *cis*-(H₂L, H₂L) arrangements of N(3)-coordinated ligands, while conformation **III** has been designated to the structure in which N(1) atom of the triazole is involved in the complex formation. The resulting geometries were checked as local minima via the harmonic frequency analysis (Table 2). The conformations **I** and **III** of complex **1** show imaginary frequencies and consequently they cannot be classified as local minima structures.

Conformation **II** has no imaginary vibrations as well as lower sum of electronic and zero-point energy values and consequently it may be characterized as a local minimum structure of the synthesized Co(II) complex. In the case of the Ni(II) complex **2**, we did not find any imaginary modes in the three optimized structures and thus the sum of the electronic and zero-point energy values was compared. As shown in Table 2, conformation **I**, incorporating two N(3)-coordinated ligands in a *trans*-arrangement, is the local minimum structure of the nickel complex. For **3**, only conformations **II** and **III** show no imaginary frequencies. Conformation **III** of the Cu(II) com-

plex is characterized as a local minimum structure because it has a lower energy value among the three optimized structures. To conclude, the complexes adapt three different conformations (Fig. 2) based on the data of the quantum chemical calculations.

Selected bond lengths and bond angles of all the optimized conformations of **1**–**3** are given in Table 3. Compounds **1**–**3** contain metal ion in a distorted tetrahedral geometry, in which the two thiourea ligands bound M²⁺ *iso*-energetically as the bonds (M–N and M–S) are equivalent. To get an insight into the distortion of the tetrahedral geometry, the four coordinated geometry index, τ_4 (Yang et al., 2007), calculated as follows, ($\tau_4 = (360 - (\alpha + \beta))/141$) (where α and β are the two largest bond angles around the central metal ion), can be applied to evaluate the distortion between the ideal four coordinated geometries; tetrahedral ($\tau_4 = 1$) and square-planar ($\tau_4 = 0$). As shown in Table 3, the τ_4 values are in the range of 0.13–0.45. The local minimum structures of complexes **1**–**3**, based on the previously mentioned vibrational analysis and ground-state energy comparison, have τ_4 values of 0.35, 0.28, and 0.45 indicating that the geometries of the complexes may be considered as an intermediate between the square planar and tetrahedral. In the case of conformation **I** of compound **2** (Fig. 2), the triazole NH group participates in intramolecular hydrogen bond with C–S–M via H–N...S with distance of 2.30922 Å, and angle of 121.1°.

The calculated vibrational spectra of the stable conformations of **1**–**3** are shown in (Fig. S4). In general, the calcu-

Table 1 The optimized proposed structures of **1**–**3**, obtained at B3LYP/def2-svp level of theory (Conformations **I**–**III** are shown from up to down).

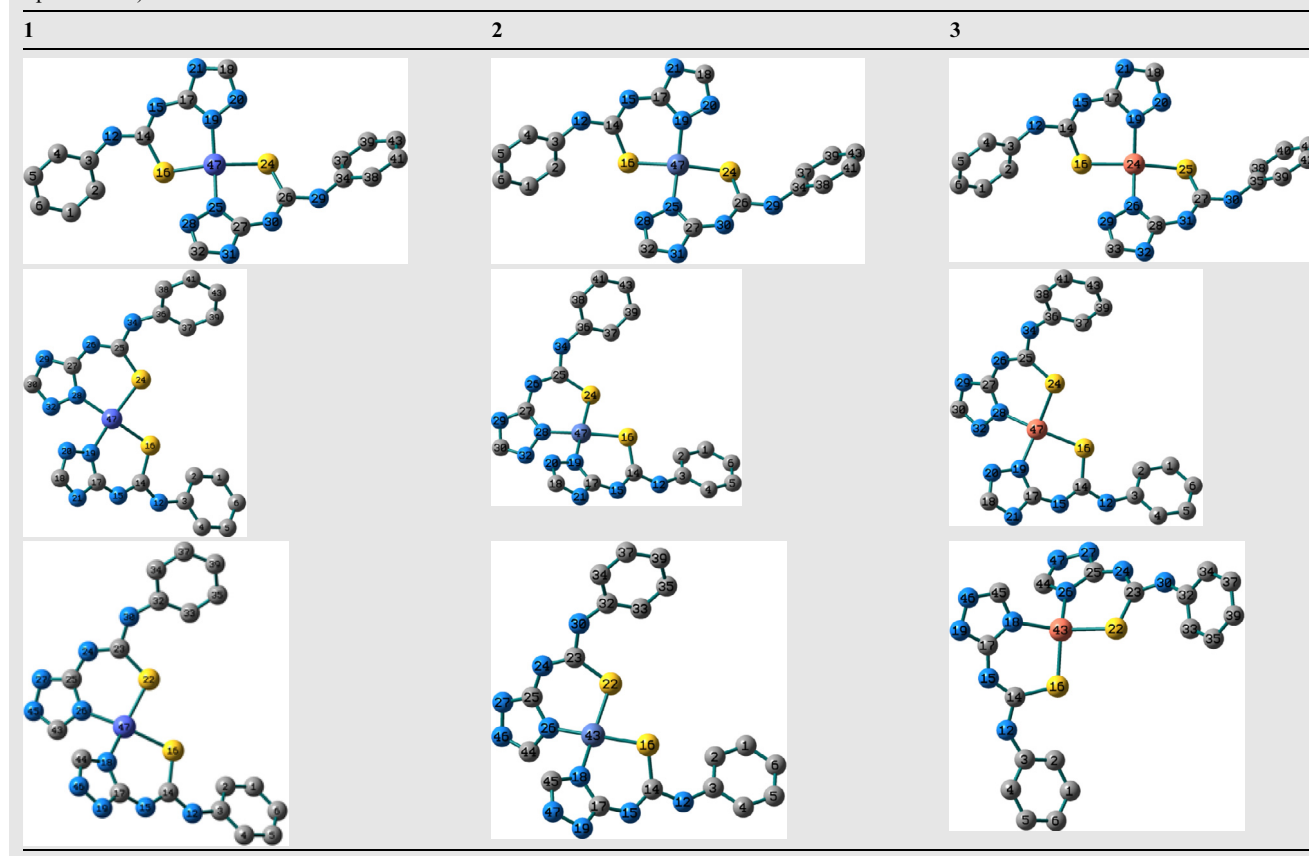


Table 2 The energy values of the proposed conformations I–III of complexes 1–3.*

	1			2			3		
	I	II	III	I	II	III	I	II	III
Electronic Energy (EE)	-1391.10107	-3421.05816	-3421.05743	-3546.59615	-3546.60879	-3546.59787	-3678.74758	-3678.73578	-3678.73819
Zero-point Energy Correction	0.494759	0.344814	0.345598	0.345432	0.345925	0.346205	0.344758	0.343773	0.344452
Thermal Correction to Energy	0.502383	0.371859	0.371520	0.372186	0.372355	0.372704	0.368529	0.371391	0.371870
Thermal Correction to Enthalpy	0.503327	0.372804	0.372464	0.373130	0.373299	0.373649	0.369473	0.372335	0.372815
Thermal Correction to Free Energy	0.456834	0.281420	0.284288	0.283764	0.284157	0.284797	0.290006	0.278956	0.279265
EE + Zero-point Energy	-1390.60631	-3420.71334	-3420.71183	-3546.25072	-3546.26286	-3546.25167	-3678.40282	-3678.39200	-3678.39374
EE + Thermal Energy Correction	-1390.59868	-3420.68630	-3420.68591	-3546.22396	-3546.23643	-3546.22517	-3678.37905	-3678.36438	-3678.36632
EE + Thermal Enthalpy Correction	-1390.59774	-3420.68535	-3420.68496	-3546.22302	-3546.23549	-3546.22422	-3678.37811	-3678.36344	-3678.36538
EE + Thermal Free Energy Correction	-1390.64423	-3420.77674	-3420.77314	-3546.31238	-3546.32463	-3546.31308	-3678.45757	-3678.45682	-3678.45893
Imaginary frequencies	32	0	1	0	0	0	4	0	0

* Conformations I, and II have been assigned to the *trans*- and *cis*-(H₂L, H₂S) arrangements of N₃-coordinated ligands, while conformation III has been designated to the structure in which N₁ atom of the triazole is involved in the complex formation.

lated wavenumbers are expected to be higher than the experimental finding because of the basis set truncation and the neglect of the electron correlation and mechanical anharmonicity especially in the range of the bending modes. (Rauhut and Pulay, 1995) To compensate these limitations, scaling methods should be introduced. Uniform scaling (0.96) was introduced for B3LYP/def2-SVP method. The scaled IR modes of NH, C = N, M–S and M–N bonds are found in the ranges of 3424–3427, 1560–1581, 356–361, and 331–342 cm⁻¹.

The natural charge, nature of bonding, type of hybridization and strength of the bonds (M–N and M–S) of the local minimum structures of 1–3 were deduced from the natural bond orbital (NBO) analysis of Weinhold and co-workers (Reed et al., 1988) and second order perturbation theory analysis of Fock Matrix in NBO Basis obtained at B3LYP/def2-SVP level of theory. The electronic arrangement of the metal center in cobalt(II) complex 1 is [Ar]4s^{0.39}3d^{7.58}4p^{0.56}5s^{0.01}, with a natural charge of 0.46222e. The occupancies of the 3d-orbitals are as follows: $d_{xy}^{0.98828} d_{xz}^{1.16688} d_{yz}^{1.64564} d_{x^2-y^2}^{1.85639} d_{z^2}^{1.92636}$. The σ (Co–S) bond is formed from sp^{6.41}d^{0.01} hybrid on S atom (a mixture of 13.48% s, 86.40% p and 0.12% d) and sp^{3.25}d^{2.29} hybrid on Co (a mixture of 32.58% s, 25.13% p and 42.29% d) and is polarized towards S atom (74.79%). Triazole nitrogen bounds metal center *via* a lone pair interaction. Both the σ (Co–S16) \rightarrow σ^* (Co–S24) and σ (Co–S24) \rightarrow σ^* (Co–S16) interactions are equal with E^2 value of 1.32 kcal mol⁻¹ (E^2 : second order interaction energy). The triazole interactions are also equal and the lone pair interaction LP(1)N19 with σ^* (Co–S24) has E^2 value of 1.73 kcal mol⁻¹. The natural charge of Ni in 2 is 0.44184e. The electronic configuration of Ni(II) ion in 2 is [Ar]4s^{0.41}3d^{8.63}4p^{0.51}5s^{0.01} and the occupancies of 3d orbitals are $d_{xy}^{1.95706} d_{xz}^{1.97954} d_{yz}^{1.95604} d_{x^2-y^2}^{0.82553} d_{z^2}^{1.91507}$. The σ (Ni–S) bond is created from sp^{7.50}d^{0.01} hybrid on S atom (comprised of 11.76% s, 88.13% p and 0.11% d) and sp^{4.05}d^{3.06} hybrid on Ni (a mixture of 12.33% s, 49.90% p and 37.76% d) and is polarized towards S atom (77.51%). The σ (Ni–S) bond is more polarized than σ (Co–S) bond because of the difference in the electronegativity between the two metal ions. The E^2 values of σ (Ni–S16) \rightarrow σ^* (Ni–S24) and LP(1)N19 \rightarrow RY*(1)Ni are 3.81 and 0.36 kcalmol⁻¹, respectively. Compared to 1, the larger the E^2 values of 2, the more intensive is the interaction between Ni(II) ion and coordination sites.

For 3, the electronic arrangement of Cu is [Ar]4s^{0.42}3d^{9.46}4p^{0.49}, the valence electrons are 10.37780 and Rydberg electrons are 0.00506. This agrees well with the natural charge on Cu ion (0.62021e), which corresponds to the difference between 28.37979e and the total number of electrons in the free copper(II) ion. The occupancies of Cu-3d subshells are $d_{xy}^{1.62771} d_{xz}^{1.97958} d_{yz}^{1.89038} d_{x^2-y^2}^{1.98588} d_{z^2}^{1.98142}$. The interactions of the nitrogen and sulphur coordination sites with Cu(II) ion may be considered as charge transfer. The E^2 values of LP(1)(S16) \rightarrow RY*(1)Cu and LP(1)N18 \rightarrow RY*(1)Cu are 0.09 and 0.23 kcalmol⁻¹, respectively.

3.3. TDDFT

The nature of the electronic absorption transitions shown in the experimental UV/Vis spectra of the local minimum structures of 1–3 has been investigated by executing time-

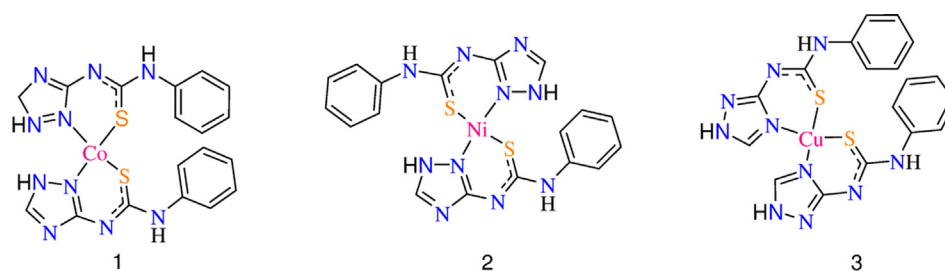


Fig. 2 Structures of the local minima structures of **1–3** based on the data of geometry optimization and vibrational analyses.

Table 3 Optimized bond length (Å) and angles (°) for conformations **I–III** of complexes **1–3** calculated B3LYP/def2-SVP level of theory (M = Co(II) (**1**), Ni(II) (**2**) and Cu(II) (**3**)).

	1			2			3		
	I	II	III	I	II	III	I	II	III
M–S	2.25726	2.23813	2.24028	2.23994	2.22476	2.22792	2.34521	2.30510	2.30562
M–N	1.92770	1.92460	1.95393	1.90674	1.90395	1.91464	1.97466	1.99974	2.01325
S–M–S	152.7	89.9	87.6	155.7	85.7	85.3	153.0	92.3	91.6
S–M–N _{in}	92.2	93.1	93.0	91.4	91.1	91.6	91.4	92.9	94.0
S–M–N _{exo}	90.9	154.8	157.5	91.9	170.4	169.4	94.3	150.9	147.9
N–M–N	166.9	94.6	95.1	164.2	93.1	93.6	155.2	96.1	97.6
τ_4^*	0.28	0.35	0.32	0.28	0.13	0.15	0.37	0.41	0.45

* ($\tau_4 = (360 - (\alpha + \beta))/141$) (where α and β are the two largest bond angles around the central metal ion).

dependent density functional theory (TDDFT) calculations. The lowest 30 singlet–singlet spin allowed excitation states were computed using CAM-B3LYP functional with long range interaction and def2-SVP basis set. The computed wavelengths including d-d transitions and their assignments are given in Table S1. In 250–800 nm range, the calculated spectrum of **1** shows two characteristic transitions at 735, and 486 nm corresponding to HOMO–4(β)/HOMO–5(β) \rightarrow LUMO(β) and HOMO–4(α) \rightarrow LUMO + 2(α), respectively. As shown in Fig. 3, the bands at 486 and 735 nm have the nature of d–d transitions.

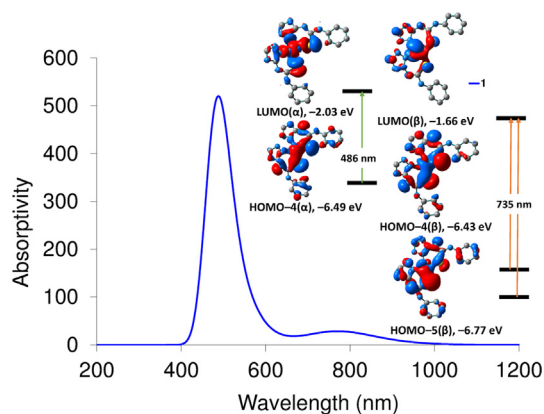


Fig. 3 Computed electronic spectrum of **1** at CAM-B3LYP/def2-SVP and frontier molecular orbitals of some selected transitions.

The TDDFT spectrum of **2** displays two main transitions at 387 and 306 nm corresponding to HOMO \rightarrow LUMO and HOMO–6 \rightarrow LUMO, respectively. As shown in Fig. 4, both HOMO and HOMO–6 orbitals are contained upon d(Ni), while LUMO is composed of π^* of phenyl ring. Thus, the transitions observed in the calculated spectrum of **2** are MLCT. The calculated spectrum of **3** shows three main transitions at 398, 317, and 269 nm corresponding to HOMO(α) \rightarrow LUMO + 1(α)/HOMO(β) \rightarrow LUMO + 2(β), HOMO–4(β) \rightarrow LUMO(β) and HOMO(β)/HOMO–2(β) \rightarrow LUMO(β). HOMO and HOMO–2 orbitals with β -spin are mainly S(π)/ligand π -

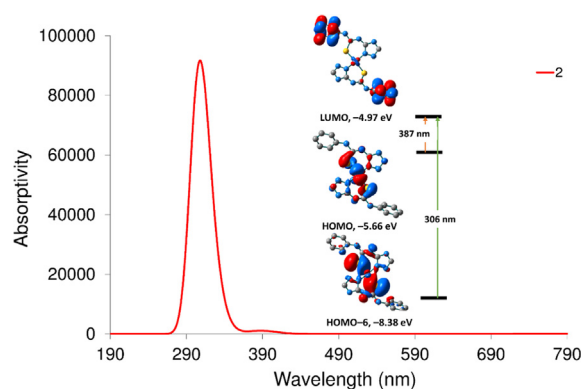


Fig. 4 Computed electronic spectrum of **2** at CAM-B3LYP/def2-SVP and frontier molecular orbitals of some selected transitions.

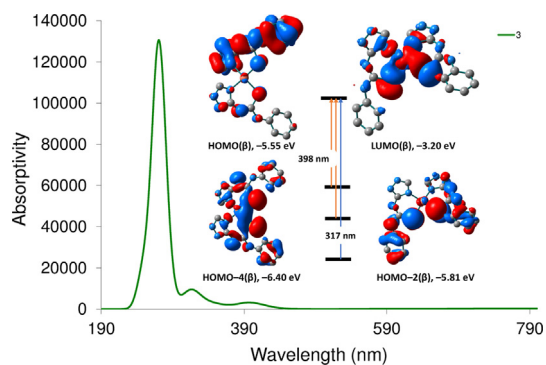


Fig. 5 Computed electronic spectrum of **3** at CAM-B3LYP/def2-SVP and frontier molecular orbitals of some selected transitions.

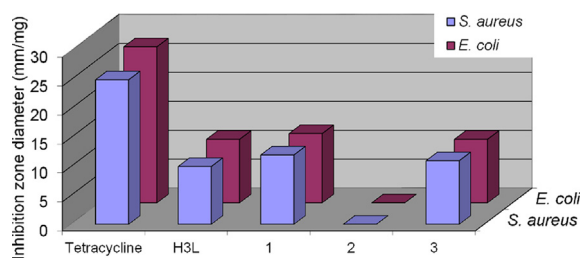


Fig. 6 Representative and comparison of the susceptibilities of *S. aureus* and *E. coli* bacteria towards the thiourea ligand and its complexes. DMSO was used as a control and its inhibition zone was withdrawing from that of each case.

orbitals (Fig. 5), whereas LUMO(β) orbital is coming from d(Cu)/S(π^*)/Triazole N(π^*). Thus, the transition at 398 nm is LMCT/LLCT. As shown in Fig. 5, the transition at 317 nm has a nature of d-d/MLCT.

3.4. Antibacterial activity

Recently, screening efforts have showed an unexpectedly high hit rate for coordination and organometallic compounds (9.9%) compared with the purely organic compounds (0.87%) submitted to the same assays. (Frei et al., 2020) Minimum inhibitory concentrations (MICs) of the tested transition metal-based compounds ($M^{n+} = \text{Mn, Co, Zn, Ru, Ag, Ir, and Pt}$) against both Gram-positive and Gram-negative bacteria were observed, with activities down to the nanomolar range against methicillin resistant *S. aureus* (MRSA). The susceptibility of *Staphylococcus aureus*, a gram-positive bacterium, and *Escherichia coli*, a gram-negative microbe, towards the free ligand and its transition metal complexes was assessed at 20 mgmL^{-1} . The potency of the compounds was compared with the standard tetracycline. The free thiourea functionalized ligand exhibits similar moderate toxicity to the tested bacteria. The possible mechanism of action of thiourea compounds functionalized with triazole moiety may be attributed to the inhibition of bacterial biofilm formation. (Stefańska et al., 2016) Coordination of the ligand to either Co(II) or Cu(II) did not alter the potency, while chelation of Ni(II) ion gives rise to inactive compound (Fig. 6). The inactivity of **2** compares well with those of Pd(II) and Pt(II) complexes of the

same ligand. (Mansour, 2018) The difference between the activities of the synthesized compounds may be attributed to the variation of the lipophilicity values, where the diffusion of the compound is low and consequently, they cannot inhibit the growth of the microbe. (Anaconda et al., 2019)

4. Conclusion

Binary metal complexes derived from reaction of N-phenyl-N'-(3-triazolyl)thiourea (H_3L) with $\text{M}(\text{ClO}_4)_2$ ($\text{M} = \text{Co(II), Ni(II) and Cu(II)}$) were synthesized in a pure form and good yield. The analytical and spectral tools showed that the thiourea ligand behaved as mono-negative *N,S*-bidentate via C-S $^-$ and triazole nitrogen affording $[\text{M}(\text{H}_2\text{L})_2]$ complexes having geometries between tetrahedral and square-planar ("flattened" tetrahedron, D_2d symmetry). The local minima structures of the proposed structures were determined with the aid of quantum chemical calculations. Analysis of the calculated vibrational spectra and comparison of the sum of the electronic and zero-point energy values of the different optimized conformations gave some knowledge about which nitrogen of the triazole ring in the complex formation (N(1) vs. N(3)) is involvement and which geometrical isomer (*cis*- vs. *trans*-) the local minimum structure is. According to the quantum chemical calculations, the complexes adapt three different conformations in which Co(II) and Ni(II) ions are coordinated to two N(3)-triazole atoms and C-S $^-$ in *cis*- and *trans*-arrangements, while Cu(II) ion is coordinated to N(1)-triazole atom and C-S $^-$ in *cis*-arrangement. Time-dependent density functional theory calculations were executed to understand the observed electronic transitions and to get an insight into the expected transitions. The ligand and its complexes were screened for their potential antibacterial activity against *Staphylococcus aureus*, and *Escherichia coli*. The free ligand exhibited similar moderate activity against the tested microbes in which the activity did not change by coordination to Co(II) and Cu(II) ions, but diminished by formation of Ni(II) complex. The possible mechanism of action of thiourea compounds functionalized with triazole moiety may be attributed to the inhibition of bacterial biofilm formation.

Author contributions

The authors have equal contribution to the present work.

Funding

The authors received no financial support for the research, authorship, and/or publication of this article.

Declaration of Competing Interest

The authors declare that they have no known competing financial interests or personal relationships that could have appeared to influence the work reported in this paper.

Appendix A. Supplementary material

Supplementary data to this article can be found online at <https://doi.org/10.1016/j.arabjc.2020.102932>.

References

- Abdel-Ghani, N.T., Mansour, A.M., 2012. Novel palladium(II) and platinum(II) complexes with 1H-benzimidazol-2-ylmethyl-N-(4-bromo-phenyl)-amine: Structural studies and anticancer activity. *Eur. J. Med. Chem.* 47, 399.
- Al-Awadi, N., Shuaib, N.M., El-Dissouky, A., 2006. Synthesis and spectroscopic characterization of nickel (II) complexes of 1-benzotriazol-1-yl-[(pX-phenyl) hydrazone] propan-2-one. *Spectrochim. Acta, Part A* 65, 36.
- Anacona, J.R., Ruiz, K., Lorono, M., Celis, F., 2019. Antibacterial activity of transition metal complexes containing a tridentate NNO phenoxymethylpenicillin-based Schiff base. An Anti-MRSA iron (II) complex. *Appl. Organomet. Chem.* 33, e4744.
- Becke, A.D., 1993. Density functional thermochemistry. III. The role of exact exchange. *J. Chem. Phys.* 98, 5648.
- Blažek Bregovic, V., Basaric, N., Mlinaric-Majerski, K., 2015. Anion binding with urea and thiourea derivatives. *Coord. Chem. Rev.* 295 (1), 80.
- K. Colanceska-Ragenovic, V. Dimova, V. Kakurinov, D. Gabor Molnar, A. Buzarovska. Synthesis, antibacterial and antifungal activity of 4-substituted-5-aryl-1, 2, 4-triazoles, *Molecules* 2001, 6, 815.
- Dhara, P.K., Pramanik, S., Lu, T., Drew, M.G.B., Chattopadhyay, P., 2004. Copper (II) complexes of new tetradentate NSNO pyridylthioazophenol ligands: synthesis, spectral characterization and crystal structure. *Polyhedron* 23, 2457.
- Dixit, P.P., Patil, V.J., Nair, P.S., Jain, S., Sinha, N., Arora, S.K., 2006. Synthesis of 1-[3-(4-benzotriazol-1-yl-2-yl-3-fluoro-phenyl)-2-oxo-oxazolidin-5-ylmethyl]-3-substituted-thiourea derivatives as antituberculosis agents. *Eur. J. Med. Chem.* 41, 423.
- Faraglia, G., Barbaro, F., Sitran, S., 1990. Palladium (II) and platinum (II) halide complexes with 2, 6-dimethyl-4H-pyran-4-thione. *Trans. Met. Chem.* 15, 242.
- Fontás, C., Hidalgo, M., Salvadó, V., Anticó, E., 2005. Selective recovery and preconcentration of mercury with benzoylthiourea-solid supported liquid membrane system. *Anal. Chim. Acta* 547, 255.
- Frei, A., Zuegg, J., Elliott, A.G., Baker, M., Braese, S., Brown, C., Chen, F., Dowson, C.G., Dujardin, G., Jung, N., King, A.P., Mansour, A.M., Massi, M., Moat, J., Mohamed, H.A., Renfrew, A.K., Rutledge, P.J., Sadler, P.J., Todd, M.W., Willans, C.E., Wilson, J.J., Cooper, M.A., Blaskovich, M.A.T., 2020. Metal complexes as a promising source for new antibiotics. *Chem. Sci.* 11, 2627.
- Frisch, M.J., Trucks, G.W., Schlegel, H.B., Scuseria, G.E., Robb, M.A., Cheeseman, J.R., Zakrzewski, V.G., Montgomery, J.A., Stratmann, R.E., Burant, J.C., Dapprich, S., Millam, J.M., Daniels, A.D., Kudin, K.N., Strain, M.C., Farkas, O., Tomasi, J., Barone, V., Cossi, M., Cammi, R., Mennucci, B., Pomelli, C., Adamo, C., Clifford, S., Ochterski, J., Petersson, G.A., Ayala, P.Y., Cui, Q., Morokuma, K., Malick, D.K., Rabuck, A.D., Raghavachari, K., Foresman, J.B., Cioslowski, J., Ortiz, J.V., Baboul, A.G., Stefanov, B.B., Liu, G., Liashenko, A., Piskorz, P., Komaromi, I., Gomperts, R., Martin, R.L., Fox, D.J., Keith, T., Al-Laham, M.A., Peng, C.Y., Nanayakkara, A., Gonzalez, C., Challacombe, M., Gill, P.M.W., Johnson, B.G., Chen, W., Wong, M.W., Andres, J.L., Head-Gordon, M., Replogle, E.S., Pople, J.A., 2003. GAUSSIAN 03 (Revision A.9), Gaussian, Inc., Pittsburgh.
- Frisch, A., Nielson, A.B., Holder, A.J., 2000. *Gaussview User Manual*. Gaussian Inc, Pittsburgh, PA.
- Fuerst, D.E., Jacobsen, E.N., 2005. Thiourea-catalyzed enantioselective cyanosilylation of ketones. *J. Am. Chem. Soc.* 124, 12964.
- Garg, B.S., Reddy, M.J., Kumar, V., 1993. Synthesis and spectroscopic studies of Cu(II) complexes of some ligands containing the amide group. *J. Coord. Chem.* 29, 33.
- Goldstein, M., Lauber, E., McKereghan, M.R., 1965. Inhibition of dopamine β -hydroxylase by some new thiourea derivatives. *J. Hid. Chew.* 240, 2066.
- Halcrow, M.A., Christou, G., 1994. Biomimetic chemistry of nickel. *Chem. Rev.* 94, 2421.
- Han, T., Cho, J.-H., Oh, C.-H., 2006. Synthesis and biological evaluation of 1 β -methylcarbapenems having cyclic thiourea moieties and their related compounds. *Eur. J. Med. Chem.* 41, 825.
- Hilal, O.M., Fredericks, G.E., 1954. Magnetic susceptibility as measured by Gouy's method with the specimen in a fixed position. *J. Chem. Soc.* 785.
- Hubbard, S.R., Till, J.H., 2000. Protein tyrosine kinase structure and function. *Rev. Biochem.* 69, 373.
- Kandil, S., Ali, G.Y., El-Dissouky, A., 2002. Cobalt (II, III) and copper (II) complexes of 3-(2-furylidene) hydrazino-5, 6-diphenyl-1, 2, 4-triazine. *Trans. Met. Chem.* 27, 398.
- Khaled, K.F., 2009. Experimental and atomistic simulation studies of corrosion inhibition of copper by a new benzotriazole derivative in acid medium. *Electrochim. Acta* 54 (18), 4345–4352.
- D. Kowalkowska-Zedler, A. Dotega, N. Nedelko, R. Łyszczek, P. Aleshkevych, I. Demchenko, J. Łuczak, A. Ślawska-Waniewska, A. Pladzyk. Structural, magnetic and spectral properties of tetrahedral cobalt (II) silanethiolates: a variety of structures and manifestation of field-induced slow magnetic relaxation, *Dalton Trans.*, 2020, 49, 697; b) A.M. Mansour, N.T. Abdel-Ghani and M.S. Ragab, *Appl. Organometal. Chem.*, 2020, 34, e5995.
- Lever, A.B.P., 1984. *Inorganic electronic spectroscopy*. Elsevier, Amsterdam.
- Liu, S.Y., Fang, L., He, Y.B., Chan, W.H., Yeung, K.T., Cheng, Y.K., Yang, R.H., 2005. Cholic-acid-based fluorescent sensor for dicarboxylates and acidic amino acids in aqueous solutions. *Org. Lett.* 7, 5825.
- Manjula, S.N., Noolvi, N.M., Parihar, K.V., Reddy, S.A.M., Ramani, V., Gadad, A.K., Singh, G., Kutty, N.G., Rao, C.M., 2009. Synthesis and antitumor activity of optically active thiourea and their 2-aminobenzothiazole derivatives: A novel class of anticancer agents. *Eur. J. Med. Chem.* 44, 2923.
- Mansour, A.M., 2013. What happens when (1H-benzimidazol-2-ylmethyl)-N-phenyl amine is added to copper (II) acetate? Spectroscopic, magnetic, and DFT studies. *Inorg. Chim. Acta* 408, 186.
- Mansour, A.M., 2014. Crystal structure, DFT, spectroscopic and biological activity evaluation of analgin complexes with Co (II), Ni (II) and Cu (II). *Dalton Trans.* 43, 15950.
- Mansour, A.M., 2016. Thermal, spectral, DFT and biological activity evaluation of Co(II), Ni(II) and Cu(II) complexes of N,S-chelated benzotriazole ligand. *J. Therm. Anal. Calorim.* 123 (1), 571–581.
- Mansour, A.M., 2018. Structural studies and biological activity evaluation of Pd (II), Pt (II) and Ru (II) complexes containing N-phenyl, N-(3-triazolyl) thiourea. *Appl. Organometal. Chem.* 32, e3928.
- Mansour, A.M., Friedrich, A., 2017. Blue-light induced CO releasing properties of thiourea based manganese (I) carbonyl complexes. *Polyhedron* 131, 13.
- Mansour, A.M., Radacki, K., 2020. Protein binding affinity of biologically active thiourea based half-sandwich Ru (II) cymene complexes. *Polyhedron* 175, 114175.
- Mansour, A.M., Shehab, O.R., 2018. Reactivity of visible-light induced CO releasing thiourea-based Mn (I) tricarbonyl bromide (CORM-NSI) towards lysozyme. *Inorg. Chim. Acta* 480, 159.
- Papakonstantinou-Garoufalas, S.S., Todoulou, O.G., Filippatos, E. C., Papadaki-Valiraki, A.E., Chytiroglou-Lada, A., 1998. Synthesis, antifungal activity and antibacterial evaluation of some 3-piperazinylmethyl-5-aryl-1H-1, 2, 4-triazoles. *Arzneimittelforschung* 1998, 48, 1019.
- Rauhut, G., Pulay, P., 1995. Transferable scaling factors for density functional derived vibrational force fields. *J. Phys. Chem.* 99, 3093.

- Reed, A.E., Curtius, L.A., Weinhold, F., 1988. Intermolecular interactions from a natural bond orbital, donor-acceptor viewpoint. *Chem. Rev.* 88, 899.
- Royer, D.J., Schivelbein, V.H., Kalyanaraman, A.F., Bertrand, J.A., 1972. The electronic structure of square-planar nickel(II) and copper(II) complexes. *Inorg. Chim. Acta* 6, 307.
- Salman, H.M.A., 2001. Spectral and thermal characterization of divalent transition metal complexes with some triazolylthiourea derivatives. *Phosphorus Sulfur Silicon Relat Elem* 173 (1), 193.
- Sreekanth, A., Kurup, M.R.P., 2003. Structural and spectral studies on four coordinate copper (II) complexes of 2-benzoylpyridine N (4), N (4)-(butane-1, 4-diyl) thiosemicarbazone. *Polyhedron* 22, 3321.
- Sreekanth, A., Prathapachandra-Kurup, M.R., 2003. Structural and spectral studies on four coordinate copper (II) complexes of 2-benzoylpyridine N (4), N (4)-(butane-1, 4-diyl) thiosemicarbazone. *Polyhedron* 22, 3321.
- Stefańska, J., Stępień, K., Bielenica, A., Szulczyk, D., Mirosalw, B., Koziol, A.E., Sanna, G., Luliano, F., Madeddu, S., Józwiak, M., Struga, M., 2016. *Med. Chem.* 12, 478.
- Stefanska, J., Szulczyk, D., Koziol, A.E., Mirosalw, B., Kedzierska, E., Fidecka, S., Busonera, B., Sanna, G., Giliberti, G., Colla, P.L., Struga, M., 2012. *Eur. J. Med. Chem.* 55, 205.
- Sundaravel, K., Suresh, E., Palaniandavar, M., 2009. Synthesis, structures, spectral and electrochemical properties of copper (II) complexes of sterically hindered Schiff base ligands. *Inorg Chim Acta* 362, 199.
- Sunduru, N., Srivastava, K., Rajakumar, S., Puri, S.K., Saxena, J.K., Chauhan, P.M.S., 2009. Synthesis of novel thiourea, thiazolidinedione and thioparabanic acid derivatives of 4-aminoquinoline as potent antimalarials. *Bioorg. Med. Chem. Lett.* 19, 2570.
- Vašák, M., Kági, J.H.R., Holmquist, B., Vallee, B.L., 1981. Spectral studies of cobalt (II)-and nickel (II)-metallothionein. *Biochem.* 20, 6659.
- Yanai, T., Tew, D.P., Handy, N.C., 2004. A new hybrid exchange-correlation functional using the Coulomb-attenuating method (CAM-B3LYP). *Chem. Phys. Lett.* 393, 51.
- Yang, L., Powell, D.R., Houser, R.P., 2007. Structural variation in copper (I) complexes with pyridylmethylamide ligands: structural analysis with a new four-coordinate geometry index, τ 4. *Dalton Trans.* 955.
- Zhao, F., Xiao, J.H., Wang, Y., Li, S., 2009. Synthesis of thiourea derivatives as CCR4 antagonists. *Chin. Chem. Lett.* 20, 296.